

# A Spectacular New Philippine Monitor Lizard: Electronic Supplemental Material

Luke J. Welton, Cameron D. Siler, Daniel Bennett, Arvin Diesmos, M. Roy Duya, Roldan Dugay, Edmund Leo B. Rico, Merlijn van Weerd, and Rafe M. Brown

There are five sections to the electronic supplemental material:

S1. Materials and Methods

S2. Supplemental Results and Discussion

- (a) *Field observations*
- (b) *Expanded description of holotype*
- (c) *Morphological variation*
- (d) *Colouration*
- (e) *Comparisons*
- (f) *Hemipeneal Morphology*
- (g) *Ecology, natural history, and diet*
- (h) *Gastrointestinal morphology*
- (i) *Distribution*
- (j) *Molecular variation and phylogeny*
- (k) *Biogeography*

S3. Acknowledgements

S4. Supplemental References

S5. Supplemental Tables

- (a) *Supplemental Table 1*
- (b) *Supplemental Table 2*
- (c) *Supplemental Table 3*

## **S1. MATERIALS AND METHODS**

Data were scored from specimens in U.S. and Philippine collections and from high-resolution photos when specimens were captured and released. Sex was determined by examination of reproductive organs and measurements (to the nearest 0.1 mm) following character definitions by Auffenberg (1988), Böhme (1988, 1991, 1995), Harvey and Barker (1998), Gaulke and Curio (2001), and Koch et al. (2007). Hemipenes of *Varanus olivaceus* (KU 322187, Polillo Island) and the holotype of *V. bitatawa* (PNM 9719, Aurora Prov., Luzon Island) were removed, everted, cleaned, retractor muscles removed, stained for 24 hours in an alizarin red solution, and then inflated with blue paraffin. Descriptive morphology follows Branch (1982), Shea and Reddacliff (1986), Böhme (1988, 1991, 1995) and Ziegler *et al.* (2007).

Molecular data were derived from all available genetic samples, including two sites at the extremes of the distribution of *V. olivaceus* and two geographically distant sites within the presumed range of the new species (Fig. 1). *Varanus mabitang* was not included because tissues for this species are unavailable. Outgroup sampling was selected from species-level molecular phylogenetic estimates (Ast, 2001), and includes new samples of *V. marmoratus*

(Luzon Island, Philippines) and *V. cumingi* (Mindanao Island, Philippines). For all samples, fragments of the 16S ribosomal RNA (16S) and NADH Dehydrogenase Subunit 1 (ND1) were sequenced, including the intervening transfer RNA (tRNA<sup>leu</sup>), following the methods of Ast (2001). Additionally we sequenced the PRLR, DNAH3, and SNCAIP nuclear protein-coding loci (Townsend et al., 2008) for four samples including exemplars of the new species, *V. olivaceus*, *V. marmoratus*, and *V. cumingi*. Genomic DNA was extracted from tissues following the guanidine thiocyanate method of Esselstyn *et al.* (2008). All sequences were deposited in GenBank under accession numbers provided in Supplemental Table 1. Primers used for amplifying mitochondrial gene sequences include: 16S–ND1 (L3827, 5'–GCAATCCAGGTCGGTTTCTATC–3' and H4644vs2, 5'–AATGGGGCTCGGTTGGTTTC–3'); PRLR (PRLR.f1, 5'–GACARYGARGACCAGCAACTRATGCC–3' and PRLR.r3, 5'–GACYTTGTGRACCTCYACRTAATCCAT–3'); DNAH3 (DNAH3.f1, 5'–GGTAAAATGATAGAAGAYTACTG–3' and DNAH3.r6, 5'–CTKGAGTTRGAHACAATKATGCCAT–3'); and SNCAIP (SNCAIP.f10, 5'–CGCCAGYTG YTG GGRAARGAWAT–3' and SNCAIP.r13, 5'–GGWGAYTTGAGDGC ACTCTTRGGRCT–3'). We used the following thermal profiles for the 16S–ND1 region: 4 min at 94°, followed by 35 cycles of 94° for 30 sec, 58° for 30 sec, and 72° for 1 min 30 sec, and a final extension phase at 72° for 7 min. For the nuclear loci, the thermal profile was identical to the profile for 16S–ND1, with the exception of having an annealing temperature of 55°. Amplified products were visualized on 1.5% agarose gels. PCR products were purified with 1 μL of a 20% dilution of ExoSAP-IT (US78201, Amersham Biosciences, Piscataway, NJ) on the following thermal profile: 31 min at 37°, followed by 15 min at 80°. Cycle sequencing reactions were run using ABI Prism BigDye Terminator chemistry (Ver. 3.1; Applied Biosystems, Foster City, CA), and purified with Sephadex Medium (NC9406038, Amersham Biosciences, Piscataway, NJ) in Centri-Sep 96 spin plates (CS-961, Princeton Separations, Princeton, NJ). Purified product was analyzed with an ABI Prism 3130xl Genetic Analyzer (Applied Biosystems). Gene sequence contigs were assembled and edited using Sequencher 4.8 (Gene Codes Corp., Ann Arbor, MI).

Initial sequence alignments were produced in Muscle (Edgar, 2004), and manual adjustments were made in MacClade 4.08 (Maddison and Maddison, 2005). To assess for possible phylogenetic incongruence between the mitochondrial and nuclear data, we inferred the phylogeny for each subset independently using likelihood and Bayesian analyses. Following no observation of statistically significant incongruence between datasets, we decided to conduct separate analyses on each locus, as well as the combined data. Exploratory analyses of the combined dataset of 27 individuals (including 23 lacking nuclear sequences) and the mitochondrial dataset (no missing data) supported identical relationships for the individuals we sequenced for nuclear loci, and we therefore chose to include all available data for subsequent analyses of the concatenated 16S–ND1 + PRLR + DNAH3 + SNCAIP dataset.

Parsimony analyses were conducted in PAUP\* 4.0b 10 (Swofford, 1999) for the combined dataset, with gaps treated as missing data and all characters weighted equally. Most parsimonious trees were estimated using heuristic searches with 1000 random addition-sequence replicates and tree bisection and reconnection (TBR) branch swapping. To assess clade confidence, nonparametric bootstrapping was conducted using 1000 bootstrap replicates, each with 100 random addition-sequence replicates and TBR branch swapping.

Partitioned Bayesian analyses were conducted in MrBayes v3.1.2 (Ronquist and

Huelsenbeck, 2003) for the combined dataset. The dataset was partitioned by 16S fragment, codon position for the protein-coding region of ND1, intervening tRNA (tRNA<sup>leu</sup>), and by nuclear loci. The Akaike Information Criterion (AIC) as implemented in Modeltest v3.7 (Posada and Crandall, 1998) was used to select the model of nucleotide substitution for each subset (Supplemental Table 2). We ran four independent Metropolis-coupled MCMC analyses, each with four chains and the default heating scheme (temp = 0.2). All analyses were run for 20 million generations, sampling every 1000 generations. To assess stationarity, all sampled parameter values and log-likelihood scores from the cold Markov chain were plotted against generation time and compared among independent runs using Tracer v1.4 (Rambaut and Drummond, 2007). All samples showed patterns consistent with stationarity after 4 million generations, hence the first 20% of samples were discarded as burn-in.

Partitioned maximum likelihood (ML) analyses were conducted in RAxMLHPC v7.0 (Stamatakis, 2006) for the combined dataset under the same partitioning strategy as for Bayesian analysis. The more complex model (GTR + I +  $\Gamma$ ) was used for all subsets, and 100 replicate ML inferences were performed for each analysis. Each inference was initiated with a random starting tree, and employed the rapid hill-climbing algorithm (Stamatakis, 2007). Clade confidence was assessed with 1000 bootstrap pseudoreplicates employing the rapid bootstrapping algorithm (Stamatakis et al., 2008).

## **S2. SUPPLEMENTAL RESULTS AND DISCUSSION**

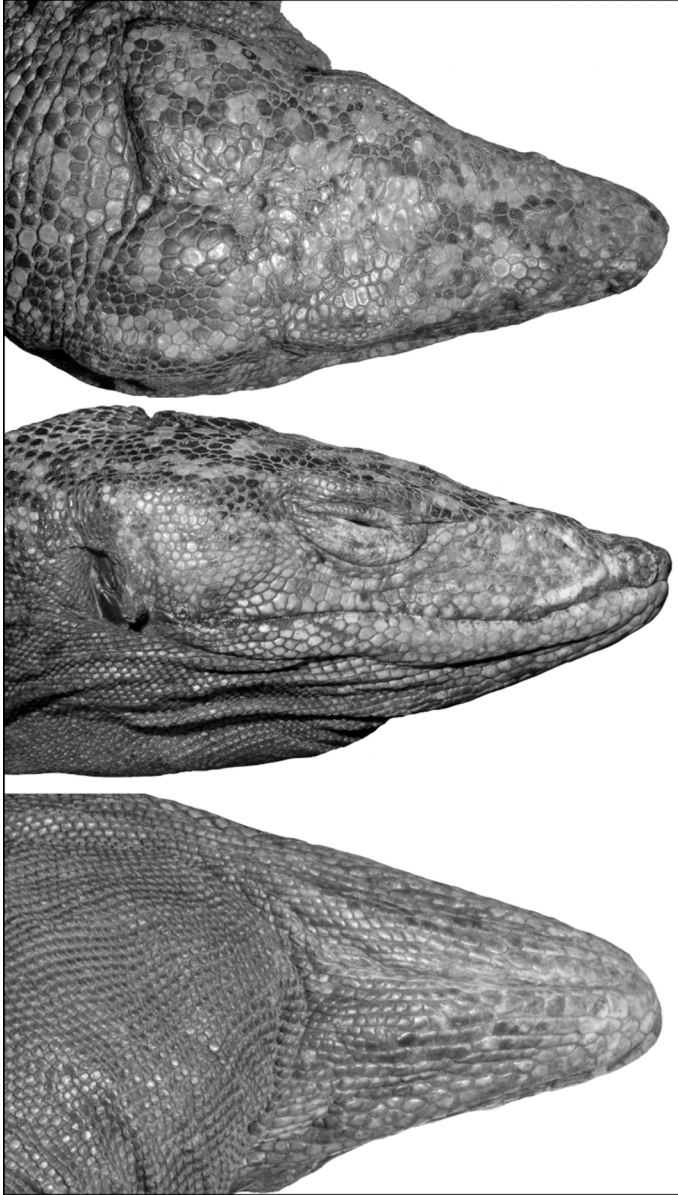
### **(a) *Field observations***

As early as 2001, evidence of a phenotypically distinct, arboreal, large-bodied, monitor lizard appeared in the form of photographed specimens circulated throughout the Philippine conservation community. The first photograph that we are aware of featured a single specimen, trapped by a local hunter and subsequently consumed by residents. Agta hunters interviewed by us in Isabela Province indicated that the local name for the species is "*bitatawa*;" in Aurora Province, Ilongot tribes' peoples refer to the new species as "*butikaw*." Subsequent surveys along the Sierra Madre range along the east coast of Luzon Island confirmed the presence of the species at numerous localities (E. L. Rico, R. Duya, L. Duya, N. A. Bartolome, U. Carestia, T. Minter, and J. Guerrero, RD, MVW, and ACD, unpublished data, 2004). In July 2005 RD collected a specimen at Sitio Dunoy, Barangay Dibulan, San Mariano, Isabela Province that was deposited at the National Museum of the Philippines (PNM 8009). Based on information from local hunters he concluded that the animal was very rarely seen. Our observations and interviews with residents in Aurora Province indicate that in some locations the new species is quite common. In interviews of Agta hunters, more than 50% of respondents claimed the "*bitatawa*" was better tasting than the "*biawak*" (*V. marmoratus*).

### **(b) *Expanded description of holotype***

Adult male, SVL 766.0 (all measurements in mm); tail 1036.0; head robust, head length 124.9, width 73.0, and maximum depth 66.8 (depth at eye 38.8); snout length 66.8, 55.5% head length; snout rounded anteriorly; narial openings 9.0, slit-like, posteriorly elevated, encircled by 11L/12R small polygonal scales; area surrounding narial opening elevated, forming distinct protuberance along canthal ridge; cranial table squarish, wider than long, with hypertrophied masseter muscle complexes enlarged and triangular in dorsal aspect.

Head scales polygonal (Supplemental Fig. 1), large, and generally homogenous in size; oculars in four semi-regular rows anterior to eye, extending posteriorly to margin of orbit; lateral head scales slightly smaller than those of dorsum, polygonal, less homogenous dorsals; dorsal and lateral head scales smooth, with shallow sutures between; supralabials 58, slightly



**Supplemental Figure 1.**— Details of head scalation in the adult male holotype of *Varanus bitatawa* (PNM 9719) in dorsal (above), lateral (middle) and ventral (below) views.

smaller than lateral head scales; infralabials 66, similar in size and shape, both series decreasing in size to rictus; nuchals large, polygonal, decreasing in size and becoming suboval to squarish laterally, and posteriorly in nuchal region; sutures between scales wider in nuchal region than on head; scales arranged in 56 semi-regular rows from posterior margin of cranial table to forelimb insertion; dorsal trunk scales slightly smaller than those of head, polygonal, becoming smaller, squarish, and more convex laterally; scales in 94 semi-regular rows through axilla–groin region; longitudinal dorsal scales (paravertebrals) 127; axilla–groin distance 272; limb scales large, polygonal, slightly convex, and decreasing in size distally; fore- and hindlimb 164 and 198 mm respectively, 21.4% and 25.8% snout–vent length, 68.8 and 81.0 diameter at insertion; digits terminating in robust, recurved claws; scales on limbs in semi-regular rows; scales of manus and pes smaller, squarish dorsally; supradigitals ovular; caudals rectangular, in semi-regular rows; ventrals less variable than dorsals; ventral head and nuchal scales heterogenous; scales small and granular anteriorly, increasing in size and becoming squarish through mid-nuchal region, then decreasing in size anterior to gular fold; scales around neck anterior to gular fold 145, mid-

gular 142; gular scales in 68 semi-regular transverse rows between gular fold and margin of tympanum; total gulars from tip of chin to gular fold, 120; trunk scales posterior to gular fold heterogenous, larger than those of nuchal region; scales in scapular region polygonal, in irregular rows, size increasing posteriorly; midbody scales in 193 semiregular rows around

trunk; ventrals from gular fold to anterior margin of hindlimb insertion 107; total ventrals from snout to hind limb insertion 227; precloacals irregular, round to polygonal slightly convex, decreasing in size distally through limbs; subcaudals heterogenous, small and granular anteriorly, increasing in size and present in semi-regular transverse rows of rectangular scales posterior to hemipeneal bulge; scales around the base of the tail 101, at one third distance from the base 59; two rows of enlarged keels (raised rectangular scales) originating 110 mm from tail base and extending posteriorly to tail terminus; terminus of tail detached.

### **(c) *Morphological variation***

Summaries of univariate morphological variation between the holotype and paratypes are presented in Table 1. Colour variation described below.

### **(d) *Colouration***

Information on variation in colour pattern (Fig. 2) is limited but our description is based on the adult holotype (PNM 9719), a juvenile paratype (KU 322188), a small adult male (PNM 9008), and photographic vouchers of three additional specimens (captured and released). Details of the holotype are as follows: dorsal surfaces brightly contrasting with black ground colour overlain by distinct, golden yellow ocelli, and a fine speckling of contrasting gold flecks; trunk with series of transverse rows of variably-sized yellow to gold ocelli; ocelli rows interspersed with smaller irregular blotches through axilla–groin region (Fig. 2); head and neck speckled yellow and black with gold blotches comprised of 1–8 scales; gular and nuchal region more melanistic, resulting in an overall darker appearance (Fig. 2); forelimbs black and yellow, distal portions with noticeably greater concentration of golden yellow than proximal portions; ventral surfaces of forelimbs faded yellow to gray; hindlimbs black with large, distinct, yellow spots on dorsal surfaces; ventral surfaces of hindlimbs speckled black and yellow; manus and pes golden yellow dorsally, with irregular aggregations of black scales; digits with 1–4 golden yellow bands; digits with single enlarged yellow terminal scale sheathing claw; palmar surface of manus black; hind-limbs similar to forelimbs; plantar surface of pes black, except for a 1–5 terminal rows of yellow; tail with 11 regular golden yellow bands from insertion to terminus, with alternating black bands containing small irregular yellow blotches; ventral surface of tail uniform faded yellow to gray; tongue pinkish gray; iris brick red.

The paratypes exhibit the same general colour pattern as the holotype but differ slightly. The juvenile paratype (KU 322188) has a nearly black gular region with 3 gray chevrons. Additionally, this specimen differs from the holotype by a reduction in the small aggregations of golden yellow spots overlaying the black portions of the dorsal pattern. The adult paratype (PNM 9008) has anterior regions of the body, neck and head, almost completely black.

In preservative, golden yellow colouration fades to pale olive. A comparison of the type series to photographs of captured and released specimens reveals that the colour pattern is fairly consistent, with some specimens exhibiting greater or lesser amounts of yellow and an occasional specimen mostly black on anterior body surfaces. Colour of the juvenile paratype and photographs of some released specimens indicate that juveniles often have a greater concentration of yellow body colouration. There is little or no ontogenetic variation in pattern in the new species, which retains its dorsal patterns and, unlike *V. olivaceus*, does not appear to fade in colour pattern with age.

### (e) *Comparisons*

The holotype of *V. bitatawa* is distinguished from the largest specimens of *V. olivaceus* by a more robust body, with thicker, more robust limbs (Fig. 2); maximum adult snout–vent length 766.0 mm, and tail length 1,036.5 mm (vs. 730.0, 1,025.0, respectively); maximum fore- and hindlimb lengths 164.1 mm and 198.7 mm (vs. 127.0 and 181.3, respectively). Additional distinguishing characteristics include a less robust head: maximum length to depth ratio 2.8 (vs. 2.4 in *V. olivaceus*); maximum nares–snout distance/snout length 0.39 (vs. 0.45); a shorter maximum tympanum–eye distance (37.8 vs. 45.1 mm); lower maximum scale count around the base of the tail (101 vs. 113); and a higher maximum number of ventrals anterior to gular fold (120 vs. 106). Distinguishing colour characteristics include dorsal ground colour black, with bright gold rows of transverse ocelli (vs. gray ground colour with brown to black transverse bands); limbs black with gold ocelli (vs. gray to black dorsum overlain with lighter random spots); juvenile gular colour gray with black chevrons (vs. chevrons absent); and brightly coloured, highly contrasting colour pattern in juveniles and adults (vs. bright, contrasting colour pattern faded in adults of *V. olivaceus*). Hemipeneal characters distinguishing *V. bitatawa* from *V. olivaceus* include an arcing, broad, primary apical hemibaculum horn (vs. hemibaculum horn flat, squarish); the presence of a short, blunt, secondary apical hemibaculum horn (vs. secondary horn sharp and pointed); and the presence (vs. absence) of a distinct evagination at the base of the primary hemibaculum (Fig. 2).

The holotype of new species is distinguished from the only adult specimens of *V. mabitang* (PNM 7272) by a considerably larger body size: mass 9 kg, SVL 766.0 mm (vs. 5.8 kg, 640 respectively); a shorter tail (1,036.5 mm vs. 1,110); shorter fore- and hindlimbs (164.1 and 198.7 mm, vs. 188.0 and 227.0 respectively); a more robust head, length to depth ratio 2.8 (vs. 2.7); narial position closer to the eye (vs. further from eye): nares–snout distance/snout length 0.39 (vs. 0.45); shorter tympanum–eye distance (37.8 vs. 42.3); fewer scales around the base of the tail (101 vs. 113); fewer midbody scale rows (193 vs. 212); fewer ventrals from gular fold to hindlimb insertion (107 vs. 124), fewer scales around the neck (120 vs 117), fewer gulars from the chin to the gular fold (145 vs. 160); dorsal trunk and limb colouration patterned black and yellow (vs. nearly uniform black); gular region patterned (vs. uniform dark gray to black).

For brevity, we do not exhaustively compare the new species to all remaining 69 species of *Varanus*. Rather, we emphasize that the new species can be distinguished from the non-frugivorous species by the same diagnostic characters used for more than a century and a half to distinguish *V. olivaceus* from other species of *Varanus* (Hallowell, 1857; Mertens, 1942; Auffenberg, 1988; Bennett, 1998; Gaulke and Curio, 2002; Pianka et al., 2004).

### (f) *Hemipeneal Morphology*

The everted hemipenis lengths of *Varanus bitatawa* and *V. olivaceus* are 63.9 and 68.1 mm respectively. Both organs (Fig. 2) are robust, differentiated into a cylindrical proximal section and a lobed, distal portion that consists of a larger primary lobe, and a smaller secondary lobe. Each lobe terminates in an ossified apical hemibaculum horn. The sulcal surface (Fig. 2) has two distinct structures in both species: the apical hemibaculum horn, at the terminus of each lobe, and a secondary out-pocketing present proximally on the primary lobe. The sulcus spermaticus of both species is basally oblique, extending distally along the sulcal surface and terminating at the bifurcation of lobes. The sulcus spermaticus is generally straight in both

species, although that of *V. bitatawa* curves away from the primary hemibaculum and that of *V. olivaceus* curves towards the primary hemibaculum. The larger, primary hemibaculum of *V. olivaceus* is terminally square, while that of *V. bitatawa* is arced, slightly concave, and nearly twice the thickness (Fig. 2). The secondary hemibaculum of *V. olivaceus* is long and conical, while that of *V. bitatawa* is significantly shorter, and cylindrical. The proximal evagination of the primary lobe has a slightly rounded protrusion in *V. olivaceus*, but a distinct, elongate, near-conical structure in *V. bitatawa*. The sulcus of *V. bitatawa* is deeper, and completely enclosed distally by the inflated lobes of the hemipenis, while that of *V. olivaceus* is shallow and barely enclosed distally, although this may be an artifact of preservation (Fig. 2). In both species, the entire hemipenis is ornamented with transverse paraphasma, or flounces, on the asulcal surface. The primary lobes of both species are adorned with eight paraphasman rows, while the secondary lobes have ten (Fig. 2). The lobes share four rows of paraphasma on the distal portion of the base, before the bifurcation of the lobes. The distal paraphasma are separated by a shallow sulcus spermaticus in *V. olivaceus*, versus a deep groove in *V. bitatawa*. The *V. bitatawa* hemipeneal structures described above are evident in both the paraffin-prepared holotype hemipenes and in the ethanol preserved everted hemipenes of the juvenile paratype (KU 322188), suggesting that the diagnostic character differences discussed here are shared by members of the new species and are not artifacts of preservation.

Due to a lack of adult female specimens, we are unable to comment on the morphology of reproductive structures in female *Varanus bitatawa*. Given the similarity between hemipenal morphology of *V. bitatawa* and *V. olivaceus*, it is likely that the homologous structures found in females will share the same level of similarity (and perhaps difference).

#### **(g) Ecology, natural history, and diet**

Little is known about the specific habits and ecology of *Varanus bitatawa*. All specimens of the new species were collected or observed deep within or on the edges of large, forested regions of the Sierra Madre Mountain Range of northeast Luzon. We strongly suspect that the new species is a forest-obligate species (like its relatives *V. olivaceus* and *V. mabitang*) and that it is heavily dependent upon unfragmented forests with sufficient stands of *Pandanus* (apparently a dominant dietary component of all frugivorous monitors). When collected at the end of June 2009 (the end of the east Luzon dry season) the holotype had *Pandanus* drupes and snail shells in its stomach; another specimen (PNM 9008) collected in July 2005 contained 11 *Pandanus* drupes. Dissections of other specimens and scat from animals held temporarily in captivity indicate a diet of *Pandanus*, *Canarium*, and *Ficus* fruits, and snails (E. L. Rico, M. R. Duya, unpublished data, 2004). These findings confirm an ecological affinity with *V. olivaceus*, a species whose diet consists almost entirely of fruit and snails (Auffenberg, 1988; Bennett, 2000). The lower digestive tract of the holotype at the time of preservation was heavily parasitized with nematodes.

#### **(h) Gastrointestinal morphology**

Our examination of the holotype's stomach and intestine confirm reports by resident hunters on dietary preferences of *Varanus bitatawa*. The digestive tract is anatomically regionalized, with the striations and out-pocketings of the stomach, the intestine anterior to the caecum, the caecum, and the intestine posterior to the caecum. The presence of a caecum and elaborate

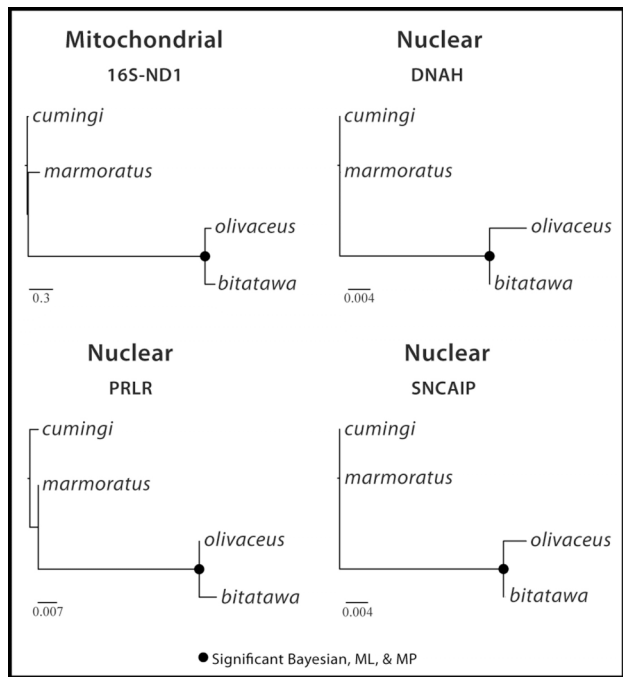
internal morphology support a conclusion of generally non-carnivorous dietary habits for this species.

**(i) Distribution**

The new species is only known from central and northern portions of the Sierra Madre range, Luzon Island, in pristine to moderately disturbed lowland and mid-elevation forests. Currently, confirmed specimens are known from the type locality of San Ildefonso Peninsula, Sitio Casapsipan, Barangay Casiguran, Municipality of Casiguran, Aurora Province, Luzon Island. The paratypes, were collected in the Lake Dunoy area, Barangay Dibuluan, Municipality of San Mariano, Isabela Province. Sight and/or photographic records include released specimens from (1) Sitio Baguio Point and Sitio Bayan, Barangay Lapi, Municipality of Peñablanca and (2) Sitio Tabugan, Barangay Santa Margarita, Municipality of Baggao (E. L. Rico and M. R. Duya, unpublished data). The forests spanning these localities (Fig. 1) can be assumed to harbor populations of *V. bitatawa*, given the presence of suitable habitat and sufficient densities of fruiting fig, *Pandanus* and *Canarium* trees.

**(j) Molecular variation and phylogeny**

The complete, aligned matrices contain 27 and 4 *Varanus* samples for the mitochondrial and nuclear datasets, respectively. Following initial unrooted analyses, we polarized the tree using samples of *V. niloticus*. Within each dataset, variable and parsimony-informative



**Supplemental Figure 2.**—Four-taxon trees pared from separate phylogenetic analyses of each locus: mitochondrial (16S, ND1) and nuclear (PRLR, DNAH3, SNCAIP) genes.

characters were observed as follows: 69/282 out of 720 for the mitochondrial data, 2/9 out of 387 for PRLR, 1/4 out of 637 for DNAH3, and 1/7 out of 480 for SNCAIP.

In mitochondrial DNA, the new species is 4.6% divergent from its closest relative, *V. olivaceus* (Table 2). Although this variation does not indicate extremely high levels of divergence between the two species, it is as great or greater than most members of the uncontroversial, morphologically distinct (*Koch et al., 2007*), widely allopatric species of the *V. salvator* group (Fig. 1; Table 2). Thus, we interpret this divergence as lending support to the hypothesis that each lineage represents a separate species. Additionally we found no intraspecific molecular divergence between the two geographically distant samples of the new species (Aurora vs. Isabela Province; Fig. 1) and no intraspecific divergence between *V. olivaceus* separated by > 200 km and the ocean channel between Luzon and Polillo Islands (Fig. 1).

Thus, we take the reciprocally monophyletic gene lineages and absence of divergence within putative species (Fig. 1) as additional evidence for the hypothesized coalescence of gene lineages, consistent with the hypothesis of speciation.

All three nuclear genes sequenced by us, although substantially less variable and informative than mitochondrial gene sequences, demonstrated identical patterns of divergence: detectable and consistent divergence between putatively distinct species. Each separate nuclear gene, when analyzed alone (Supplemental Fig. 2) lends support from independent gene loci to the observation of molecular divergence between *V. olivaceus* and the new species (Supplemental Table 3).

Analyses of the combined data (16S–ND1 + PRLR + DNAH3 + SNCAIP) resulted in topologies with mixed bootstrap support (MP and ML) and posterior probabilities (Supplemental Fig. 2). Topologies were congruent across these analyses, and parsimony and likelihood bootstrapping analyses and posterior probability in Bayesian analyses all consistently showed high support for the sister relationship between *Varanus olivaceus* and *V. bitatawa* (Figure 1).

### **(k) Biogeography**

The new species appears to be separated from its closest relative, *V. olivaceus*, by a distributional gap of greater than 150 km. This gap in the known ranges of two species is crossed by no fewer than three proposed barriers to dispersal (Fig. 1: low elevation, arid, unforested valleys) and also coincides with division of the two main geological components of the Sierra Madre on either side of the Lingayen-Dingalan fault zone (Defant et al., 1989; Yumul et al., 2003). The coincidence between *Varanus* species distributions and the boundaries of the geological components of Luzon lends support to the hypothesis that the divergence of the two species may be related to geological processes that bisected today's apparently contiguous Sierra Madre Range (Auffenberg, 1988; Hall, 2002; Yumul et al., 2009).

Aside from ancient geological events (Yumul et al., 2003, 2009), purely ecological factors may drive species divergence. As we conceive of it, the Mid-Sierra Filter Zone hypothesis predicts that if low elevation, arid non-forested valleys serve as barriers to dispersal for obligate montane forest species, then patterns of genetic divergence and geographical structure should geographically coincide in unrelated taxa across the proposed barriers subdividing the Sierra Madre Mountain Range (Fig. 1). This hypothesis provides fertile ground for future phylogeographic and conservation genetic studies. If supported with data from other taxa, recognition of the Mid-Sierra Filter Zone may require revision of prevailing conservation and management strategies that currently treat the Sierra Madre as a single, contiguous corridor of relatively uninterrupted habitat. Thus, the "Sierra Madre Corridor" may actually represent two or more sub-centers of endemism, each of which might best be managed separately.

### **S3. ACKNOWLEDGEMENTS**

Support for fieldwork was provided by the University of Kansas, National Museum of the Philippines, National University of Singapore, Rufford Small Grants Foundation (171/07/04 to ACD), North of England Zoological Society, Dallas Zoo, Conservation International, the Cagayan Valley Program on Environment and Development, and the U.S. National Science Foundation (DEB 0743491 to RMB). We thank the Philippines' Department of Environment and Natural Resource for facilitating research and export permits and the Local Government Units of Peñablanca, Baggao, Cagayan, Maconacon, and San Mariano for their cooperation.

We thank J. Siler, J. Brown, N. Antoque, D. Afan, M. Quilala, H. Garcia, E. Jose, and M. and Adonis Diesmos, and V. and M. Yngente for assistance in the field and D. Blackburn and an anonymous reviewer for critical review. Thanks to L. Trueb for assistance with figures. Liza Duya, N. Bartolome, T. Headland, U. Carestia, S. Telan, W. Oliver, R. Sison, T. Minter, J. Guerrero graciously shared observations and data.

#### S4. SUPPLEMENTAL REFERENCES

- Ast, J. 2001 Mitochondrial DNA evidence and evolution in Varanoidea (Squamata). *Cladistics* **17**, 211–226.
- Bennett, D. 2000 Status report for *Varanus olivaceus* on Polillo Island. In Wildlife of Polillo Island, Philippines (ed. Bennett, D.), pp. 1–38. Glossop: Viper Press.
- Bennett, D. 2009 How does *Varanus olivaceus* alter seed shadows of the plants it feeds on? The effects of frugivory on seed dispersal. Doctoral Dissertation, University of Leeds.
- Böhme, W. 1988 Zur Genitalmorphologie der Sauria: funktionelle und stammesgeschichtliche Aspekte. *Bonn Zool. Monogr.* **3**, 1–76
- Böhme, W. 1991 New findings on the hemipenal morphology of monitor lizards and their systematic implications. *Mertensiella.* **2**, 42–49
- Böhme W. 1995 Hemiclitoris discovered: a fully differentiated erectile structure in female monitor lizards (*Varanus* spp.) (Reptilia: Varanidae). *J. Zoo. Syst. Evol. Research.* **33**, 129–132.
- Branch, W. R. 1982 Hemipeneal morphology of platynotan lizards. *J. Herpetol.* **16**, 16–38.
- Defant, M. J., Jacques, D., Maury, R. C., De Boer, J., & Joron, J.-L. 1989 Geochemistry and tectonic setting of the Luzon arc, Philippines. *Geol. Soc. America Bull.* **101**, 663–672.
- Edgar, R.C. 2004 MUSCLE: multiple sequence alignment with high accuracy and high throughput. *Nuc. Acid Res.* **32**, 1792–1797.
- Esselstyn, J. A., Garcia, H. J. D., Saulog, M. G., & Heaney, L. R. 2008 A new species of *Desmalopex* (*Pteropodidae*) from the Philippines, with a phylogenetic analysis of the Pteropodini. *J. Mammal.* **89**, 815–825.
- Gray, J.E. 1845 Catalogue of the specimens of lizards in the collection of the British Museum. London: Trustees of the British Museum.
- Günther, A. 1872 On two species of *Hydrosaurus* from the Philippine Islands. *Proc. Zool. Soc. London* **1872**, 145–146.
- Hallowell, E. 1857. Notes on the Reptiles in the collection of the Museum of the Academy of Natural Sciences, Philadelphia. *Phil. Sci. Bull.* **8**, 146–153.
- Koch, A., Auliya, M., Schmitz, A., Kuch, U., & Böhme, W. 2007 Morphological studies on the systematics of South East Asian water monitors (*Varanus salvator* Complex): nominotypic populations and taxonomic overview. *Mertensiella* **16**, 109–180.
- Macey, J. R., Wang, Y., Ananjeva, N. B., Larson, A. & Papenfuss, T. J. 1999 Vicariant patterns of fragmentation among Gekkonid lizards of the genus *Teratoscincus* produced by the Indian collision: A molecular phylogenetic perspective and an area cladogram for central Asia. *Mol. Phylo. Evol.* **12**, 320–332.
- Maddison, D. R., Maddison, W. P. 2005 MacClade: analysis of phylogeny and character evolution, Version 4.08. Sunderland: Sinauer Associates.
- Martin, W. C. L. 1839 Remarks on two species of saurian reptiles. *Proc. Zool. Soc. London* **64**, 68–70 .

- Posada, D., Crandall, K. A. 1998 Modeltest: testing the model of DNA substitution. *Bioinformatics* **14**, 817–818.
- Rambaut, A., Drummond, A. J. 2007 Tracer v1.4. Available at <http://beast.bio.ed.ac.uk/Tracer>.
- Ronquist, F., Huelsenbeck, J. P. 2003 MRBAYES 3: Bayesian phylogenetic inference under mixed models. *Bioinformatics* **19**, 1572–1574.
- Shea, G. M., and G. L. Raddacliffe. 1986. Ossifications in the hemipenes of varanids. *J. Herpetol.* **20**, 566–568.
- Stamatakis, A., 2006 RAxML-VI-HPC: maximum likelihood-based phylogenetic analyses with thousands of taxa and mixed models. *Bioinformatics* **22**, 2688–2690.
- Stamatakis, A., Blagojevic, F., Nikolopoulos, D., Antonopoulos, C. 2007 Exploring new search algorithms and hardware for phylogenetics: RAxML meets the IBM cell. *J. VLSI Signal Proc.* **48**, 271–286.
- Stamatakis, A., Hoover, P., Rougemont, J. 2008 A rapid bootstrap algorithm for the RAxML Web Servers. *Sys. Biol.* **57**, 758–771.
- Swofford, D.L. 1999 PAUP\*4.0. Phylogenetic analysis using parsimony (\*and other methods). Sunderland: Sinauer Associates.
- Townsend, T. M., Alegre, R. E., Kelley, S. T., Wiens, J. J., and Reeder, T. W. 2008 Rapid development of multiple nuclear loci for phylogenetic analysis using genomic resources: An example from squamate reptiles. *Molec. Phylo. Evol.* **47**, 129–142.
- Wiegmann, A. F. A. 1834 Beiträge zur Zoologie gesammelt auf einer Reise um die Erde. Siebente Abhandlung. Amphibien. *Nova Acta Acad. Caesar. Leop. Carol., Halle* **17**, 185–268.
- Yumul, G. P. Jr., Dimalanta, C. B., Tamayo, R. A. Jr., & Maury, R. C. 2003 Collision, subduction and accretion events in the Philippines: A synthesis. *The Island Arc* **12**, 77–91.

## S5. SUPPLEMENTAL TABLES

(a) *Supplemental Table 1*.—Summary of specimens corresponding to genetic samples included in the study, general locality, and GenBank accession numbers.

Species	Voucher	Locality	Genbank Accession Numbers			
			16S–ND1	PRLR	DNAH3	SNCAIP
<i>Varanus timorensis</i>	WAM R107008	Timor, Semau, Savu	AF407532	–	–	–
<i>Varanus rosenbergi</i>	No voucher	Southern Australia	AY264941	–	–	–
<i>Varanus mertensi</i>	AM R123877	Northern Australia	AF407512	–	–	–
<i>Varanus komodoensis</i>	Zoo specimen	Komodo Island, Indonesia	AF407510	–	–	–
<i>Varanus keithhornei</i>	QM 70792	Northeast Australia	AF407508	–	–	–
<i>Varanus beccari</i>	UMFS 10371	Aru islands, Indonesia	AF407490	–	–	–
<i>Varanus salvator togianus</i>	UMFS 10298	No locality data	AF407524	–	–	–
<i>Varanus salvator bivitatus</i>	UMFS 10670	Java Island, Indonesia	AF407525	–	–	–
<i>Varanus salvator salvator</i>	No voucher	No locality data	AF407526	–	–	–
<i>Varanus prasinus</i>	UMFS 10684	Papua New Guinea	AF407519	–	–	–
<i>Varanus jobiensis</i>	UMMZ 211713	Papua New Guinea	AF407507	–	–	–
<i>Varanus indicus</i>	AM 36431	Northern Australia or New Guinea	AF407506	–	–	–
<i>Varanus indicus</i>	AM 51525	New Guinea	AF407504	–	–	–
<i>Varanus indicus</i>	AM R137997	Indonesia	AF407505	–	–	–
<i>Varanus doreanus</i>	UMFS 10296	Papua New Guinea	AF407493	–	–	–
<i>Varanus melinus</i>	UMFS 10164	Indonesia	AF407511	–	–	–
<i>Varanus yuwonoi</i>	UMMZ 225545	Halmaherra island, Indonesia	AF407535	–	–	–
<i>Varanus niloticus</i>	UMMZ 221377	South Africa or Central Africa	AF407514	–	–	–
<i>Varanus brevicauda</i>	No voucher	Australia	AY264940	–	–	–
<i>Varanus bitatawa</i>	KU 322188	Philippines, Luzon Island, Isabela Province, Municipality of San Mariano, Barangay Dibuluan, Sitio Dunoy	HM017191, HM017196	–	–	–
<i>Varanus bitatawa</i>	PNM 9719	Philippines, Luzon Island, Aurora Province, Municipality of Casiguran, Barangay Casiguran, Sitio Casapsipan,	HM017192, HM017197	HM017205	HM017201	HM017209
<i>Varanus olivaceus</i>	KU 322187	Philippines, Polillo Island, Quezon Province, “East Polillo”	HM017193, HM017198	HM017206	HM017202	HM017210
<i>Varanus olivaceus</i>	KU 322186	Philippines, Luzon Island, Camarines Sur Province, Caramoan Peninsula	HM034754, HM034755	–	–	–
<i>Varanus marmoratus</i>	KU 322191	Philippines, Occidental Mindoro Province, Lubang Island, Municipality	HM017194, HM017199	HM017207	HM017203	HM017211
<i>Varanus cumingi</i>	KU 321814	Philippines, Zamboanga City Province, Pasonanca Natural Park	HM017195, HM017200	HM017208	HM017204	HM017212

**(b) Supplemental Table 2.**—Models of evolution selected by AIC and applied for partitioned, Bayesian phylogenetic analyses<sup>1</sup>.

Partition	AIC Model	Number of Characters
16S	HKY + G	59
tRNA <sup>Leu</sup>	GTR + G	74
ND1, 1 <sup>st</sup> codon position	GTR + G	196
ND1, 2 <sup>nd</sup> codon position	GTR + I + G	196
ND1, 3 <sup>rd</sup> codon position	GTR + I + G	195
PRLR	HKY	387
DNAH	GTR	637
SNCAIP	GTR	480

<sup>1</sup>The model GTR + I + G was used for partitioned RAxMLHPC analyses.

**(c) Supplemental Table 3.**—Uncorrected pairwise sequence divergence (%) for nuclear data for *Varanus bitatawa*, *V. olivaceus*, *V. marmoratus*, and *V. cumingi*. In each cell, sequence divergences are shown for PRLR, DNAH3, SNCAIP (top to bottom, respectively), and total nuclear sequence divergence (bolded for emphasis).

	<i>bitatawa</i>	<i>olivaceus</i>	<i>marmoratus</i>	<i>cumingi</i>
<i>bitatawa</i>	—			
	0.3			
<i>olivaceus</i>	0.2	—		
	0.2			
	<b>(0.2)</b>			
	2.8	2.3		
<i>marmoratus</i>	0.6	0.8	—	
	1.5	1.7		
	<b>(1.4)</b>	<b>(1.5)</b>		
	2.8	2.6	0.3	
<i>cumingi</i>	0.6	0.8	0.0	—
	1.5	1.7	0.0	
	<b>(1.5)</b>	<b>(1.5)</b>	<b>(0.1)</b>	